



## Selective fluorescence and naked eye detection of histidine in aqueous medium via hydrogen bonding assisted Schiff base condensation



Sisir Lohar<sup>a</sup>, Arnab Banerjee<sup>a</sup>, Animesh Sahana<sup>a</sup>, Sukanya Panja<sup>b</sup>, Ipsit Hauli<sup>b</sup>, Subhra Kanti Mukhopadhyay<sup>b</sup>, Debasis Das<sup>a,\*</sup>

<sup>a</sup> Department of Chemistry, The University of Burdwan, Burdwan 713104, West Bengal, India

<sup>b</sup> Department of Microbiology, The University of Burdwan, Burdwan 713104, West Bengal, India

### ARTICLE INFO

#### Article history:

Received 11 September 2013

Revised 27 October 2013

Accepted 29 October 2013

Available online 6 November 2013

#### Keywords:

Visible light excitation

Naked eye

Histidine

Cell imaging

DFT

### ABSTRACT

Visible light excitable rhodamine B derivative (**TARDHD**) has been developed for fluorescence and naked eye detection of histidine in aqueous medium. **TARDHD** shows 45 fold fluorescence enhancement in the presence of histidine. It forms Schiff base with histidine and stabilizes via intra-molecular H-bonding. **TARDHD** can efficiently detect intracellular histidine.

© 2013 Elsevier Ltd. All rights reserved.

Among several essential amino acids, histidine is actively involved in human growth, and acts as a neurotransmitter in the central nervous system.<sup>1,2</sup> Deviation from its normal level leads to different diseases including chronic kidney problems having impaired nutritional state.<sup>3,4</sup> Recently, several probes for selective detection of amino acid viz. cysteine and homocysteine,<sup>5</sup> lysine,<sup>6</sup> arginine (Arg),<sup>7</sup> phenylalanine (Phe)<sup>8</sup> and tryptophan<sup>9</sup> have been reported. Among a few histidine (His)<sup>10,11</sup> selective fluorescence sensors, mostly suffer interferences either from cysteine, lysine, arginine<sup>12</sup> or any other amino acids.<sup>13</sup> Lin Pu group have used terpyridine based Cu(II)<sup>14</sup> and Zn(II)<sup>15</sup> complexes as fluorescence sensors for histidine. However, the former suffer interference from cysteine and the latter lacks in quantum yield, lowest detection limit, cell imaging studies and theoretical support. Most importantly, both the sensors require excitation with undesirable UV light and hence, unworthy for intracellular studies. Interestingly, till date, naked eye detection of histidine remains unexplored. We have overcome these limitations and report a very simple rhodamine-based visible light excitable ON type fluorescence probe, **TARDHD** for selective, naked eye determination of histidine under physiological condition. Rhodamine-based fluorescent probes are chosen for recognition of amino acids<sup>5a</sup> for their excellent

spectroscopic properties, viz. high molar extinction coefficient ( $\epsilon$ ) and fluorescence quantum yield ( $\Phi$ ). Facile synthesis of **TARDHD** has been achieved by two-step reaction using rhodamine B and phthalaldehyde as shown in Scheme S1 (Supplementary data, hereafter ESI). First, rhodamine B is refluxed with hydrazine hydrate for 3 h in ethanol to afford rhodamine-hydrazine adduct, **2** in 97% yield following a literature procedure.<sup>16</sup> Then, **2** is reacted with phthalaldehyde to get **TARDHD** in 75% yield. It is characterized by <sup>1</sup>H NMR, QTOF-MS, FTIR spectra and elemental (CHN) analysis (Figs. S1, S2, and S3, ESI). The colourless non-fluorescent state of **TARDHD** indicates its spirolactam ring structure.

**TARDHD** (10  $\mu$ M) undergoes 45 fold fluorescence enhancement upon addition of 100 equivalent of histidine in HEPES buffered (0.1 M) solution (ethanol/water, 1:9, v/v, pH 7.3,  $\lambda_{\text{Ex}} = 560$  nm,  $\lambda_{\text{Em}} = 601$  nm). Changes in the emission profile of **TARDHD** upon gradual addition of histidine are presented in Figure S4 (ESI). The results clearly indicate that the spirolactam ring opens with the formation of a highly conjugated structure (Fig. 1). The fluorescence quantum yields ( $\Phi_{\text{F}}$ ) of **TARDHD** and its histidine adduct are 0.007 and 0.12, respectively where rhodamine B is used as standard ( $\Phi_{\text{F}} = 0.65$  in ethanol).<sup>17</sup> Job's plot (Fig. S5, ESI) shows 1:1 (mole ratio) stoichiometry of the **TARDHD**–histidine adduct. ESI-TOF (+) mass spectrum (Fig. S6, ESI) also supports the formation of **TARDHD**–histidine Schiff base having  $m/z$  at 710.47 [**TARDHD** + histidine – H<sub>2</sub>O + H<sup>+</sup>]. FTIR spectrum (Fig. S2, ESI) of free

\* Corresponding author. Tel.: +91 342 2533913; fax: +91 342 2530452.

E-mail address: [ddas100in@yahoo.com](mailto:ddas100in@yahoo.com) (D. Das).

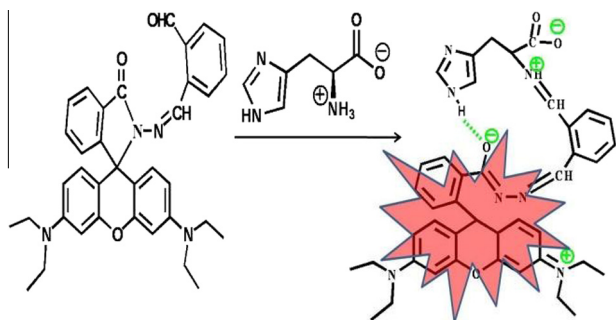


Figure 1. Proposed mechanism of histidine sensing with TARDHD.

TARDHD shows peaks at 1730, 1691 and 1615  $\text{cm}^{-1}$  corresponding to carbonyl stretching from aldehyde, ketone and imine ( $\text{CH}=\text{N}$ ) functionalities.

In Schiff base adduct (Fig. S7, ESI), 1730  $\text{cm}^{-1}$  peak disappears with the appearance of a new broad peak at 3386  $\text{cm}^{-1}$ , assigned to imidazole N–H stretching of histidine residue.

The binding constant of TARDHD for histidine is  $3.7 \times 10^4 \text{ M}^{-1}$  (Fig. S8, ESI), as estimated using the following Benesi–Hildebrand equation:<sup>18</sup>

$$F_{\text{lim}} - F_0/F_x - F_0 = 1 + (1/K[C]^n) \quad (1)$$

where  $F_0$ ,  $F_x$  and  $F_{\text{lim}}$  are the emission intensities of TARDHD in absence of histidine, at an intermediate histidine concentration, and at histidine concentration of complete interaction respectively.  $K$  is the binding constant,  $C$  is the concentration of histidine and  $n$  is the number of histidine molecules bound per TARDHD molecule (here  $n = 1$ ). Lowest detection limit for histidine is  $1.1 \times 10^{-8} \text{ M}$  (Fig. S9, ESI). Figure 2 reveals that TARDHD has no absorbance in the visible region. In presence of histidine, a new absorption peak appears at 560 nm, the intensity of which increases with increasing histidine concentration. This allows naked eye detection and colorimetric determination of histidine. Figure S10 (ESI) shows UV–vis titration of TARDHD with histidine which provides the binding constant,  $2.8 \times 10^4 \text{ M}^{-1}$ , in close agreement to the value derived from fluorescence titration.

The sensing of mechanism is attributed to the formation of TARDHD–histidine Schiff base followed by its stabilization through H-bonding involving carbonyl oxygen of rhodamine unit and imidazole N–H of histidine residue.

Free imidazole fails to show fluorescence enhancement of TARDHD. Similarly, other amino acids do not interfere (Figs. S11

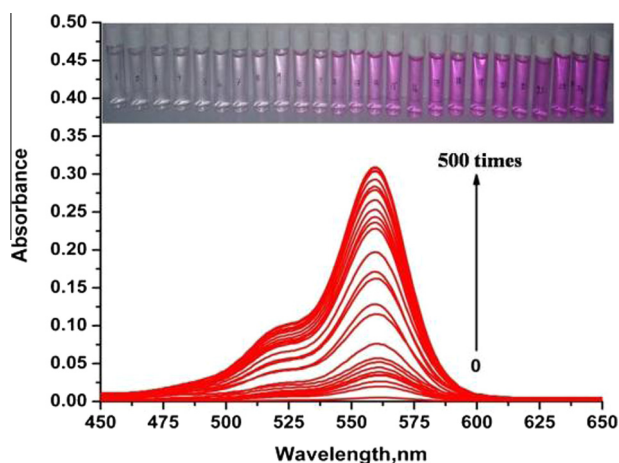


Figure 2. Changes of absorbance of TARDHD (10  $\mu\text{M}$ ) upon addition of histidine (0, 1, 5, 10, 15, 20, 40, 50, 80, 100, 150, 200, 250, 300, 400, 500, 700, 800, 1000, 2000 and 5000  $\mu\text{M}$ ) in HEPES buffered (0.1 M) solution (ethanol/water = 1:9, v/v, pH 7.3).

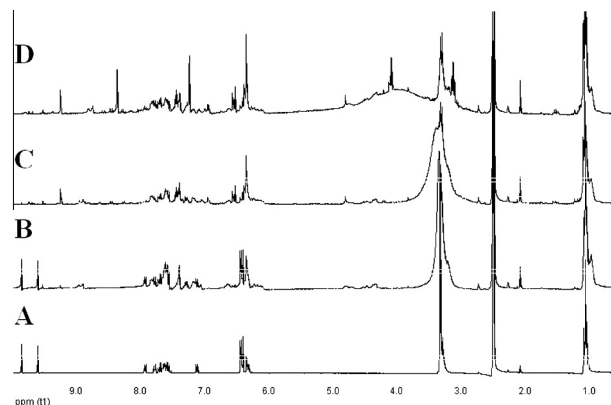


Figure 3.  $^1\text{H}$  NMR spectral changes of TARDHD upon gradual addition of histidine: (A) free TARDHD, (B) TARDHD in MeOD + 0.5 equiv histidine in  $\text{D}_2\text{O}$ , (C) TARDHD in MeOD + 1 equiv histidine in  $\text{D}_2\text{O}$ , (D) TARDHD in MeOD + 2 equiv histidine in  $\text{D}_2\text{O}$ .

and Fig. S12, ESI). This indicates that neither hydrogen bonding nor Schiff base formation is individually responsible for fluorescence enhancement. Their combined effect is essential for turning on the fluorescence via ring opening of TARDHD.

Interaction between TARDHD and histidine has been monitored by  $^1\text{H}$  NMR titration in  $\text{D}_2\text{O}/\text{CD}_3\text{OD} = 1:9$  (v/v) (Fig. 3). The aldehyde proton at 9.85 ppm of free TARDHD disappears upon addition of 1 equiv histidine indicating Schiff base formation. Imine proton ( $\text{CH}=\text{N}$ ) of free TARDHD have shifted from 9.59 to 9.23 ppm and merges to the new imine proton formed due to Schiff base formation with histidine. Imidazole ring N–H proton, exchangeable with  $\text{D}_2\text{O}$  does not appear, however, imidazole ring  $-\text{CH}_2$  and  $-\text{N}=\text{CH}$  protons which generally appear at 7.12 ppm and 8.08 ppm in free histidine have been shifted to 7.23 and 8.35 ppm upon reaction with TARDHD.

Density functional theoretical studies (DFT, B3LYP/6-311G basis set)<sup>19</sup> provide additional support to the histidine sensing mechanism. Figure 4 reveals that HOMO–LUMO energy gap in free TARDHD and its histidine adduct are 3.107 and 2.695 eV respectively. Moreover, in HOMO of TARDHD, most of the charge resides in the rhodamine moiety but in LUMO, it is on the phthalaldehyde unit. In TARDHD–histidine adduct, most of the charges relocate on phthalaldehyde unit in both HOMO and LUMO. Most importantly, it indicates a strong H-bond (2.436 Å) between ketone oxygen of rhodamine moiety with imidazole N–H from histidine residue (Fig. 5).

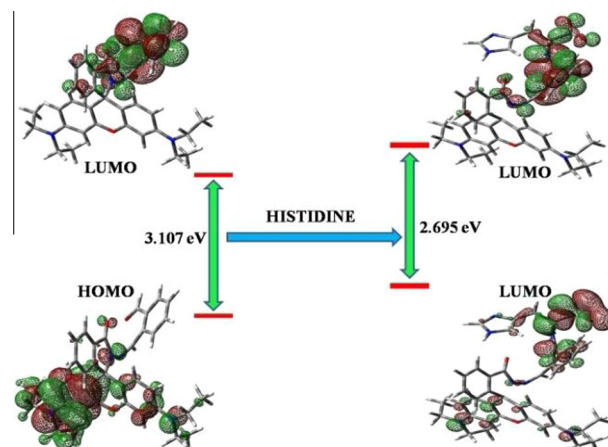
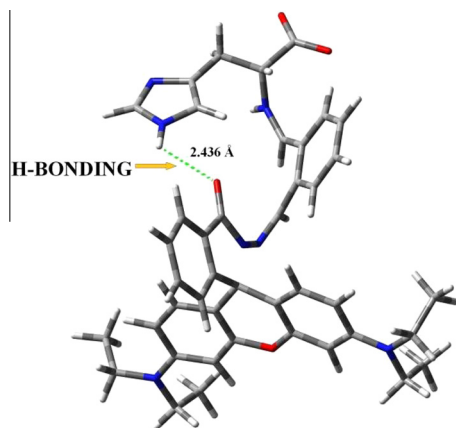


Figure 4. Energy optimized structure and HOMO–LUMO energy gap of TARDHD and its Schiff base with histidine.



**Figure 5.** Stereoscopic view of the optimized H-bonded structure of TARDHD + histidine adduct.

4–9, it is suitable for histidine sensing. However, pH 7.3, being physiological pH is chosen for the entire studies.

Figure 6 and Figure S14 (ESI) clearly show that the probe is easily permeable to the tested living cells and harmless (as the cells remain alive even after a considerable time of exposure to the probe).

A very simple visible light excitable fluorescent probe for naked eye detection of histidine in aqueous medium is reported. The probe has a very good lowest LOD and capable to detect intracellular histidine without any interference.

### Acknowledgments

S.L, A.B. and A.S. are grateful to CSIR, New Delhi for providing fellowship. We sincerely thank USIC, Burdwan University for providing fluorescence facilities.

### Supplementary data

Supplementary data associated with this article can be found, in the online version, at <http://dx.doi.org/10.1016/j.tetlet.2013.10.144>.

### References and notes

- (a) Kopple, J. D.; Swendseid, M. E. *J. Clin. Invest.* **1975**, *55*, 881; (b) Snyderman, S. E.; Boyer, A.; Roitman, E.; Holt, L. E., Jr.; Prose, P. H. *Pediatrics* **1963**, *31*, 786.
- Kusakari, Y.; Nishikawa, S.; Ishiguro, S.-i.; Tamai, M. *Curr. Eye Res.* **1997**, *16*, 600.
- Watanabe, M.; Suliman, M. E.; Qureshi, A. R.; Garcia-Lopez, E.; Bárány, P.; Heimbürger, O.; Stenvinkel, P.; Lindholm, B. *Am. J. Clin. Nutr.* **2008**, *87*, 1860.
- (a) Jones, A. L.; Hulett, M. D.; Parish, C. R. *Immunol. Cell Biol.* **2005**, *83*, 106; (b) Sullivan, D. J., Jr.; Gluzman, I. Y.; Goldberg, D. E. *Science* **1996**, *271*, 219; (c) Leebeek, F. W. G.; Kluff, C.; Knot, E. A. R.; De Maat, M. P. M. *J. Lab. Clin. Med.* **1989**, *113*, 493; (d) Saito, H.; Goodnough, L. T.; Boyle, J. M.; Heimbürger, N. *Am. J. Med.* **1982**, *73*, 179.
- (a) Yang, Y.-K.; Shim, S.; Tae, J. *Chem. Commun.* **2010**, 7766; (b) Hao, W.; McBride, A.; McBride, S.; Gao, J. P.; Wang, Z. Y. *J. Mater. Chem.* **2011**, *21*, 1040; (c) Chen, X.; Zhou, Y.; Peng, X.; Yoon, J. *Chem. Soc. Rev.* **2010**, *39*, 2120.
- (a) Wehner, M.; Schrader, T.; Finocchiaro, P.; Failla, S.; Consiglio, G. *Org. Lett.* **2000**, *2*, 605; (b) Sasaki, S.; Hashizume, A.; Citterio, D.; Fujii, E.; Suzuki, K. *Tetrahedron Lett.* **2002**, *43*, 7243; (c) Secor, K.; Plante, J.; Avetta, C.; Glass, T. J. *Mater. Chem.* **2005**, *15*, 4073; (d) Mandl, C. P.; König, B. *J. Org. Chem.* **2005**, *70*, 670.
- Liu, K.; He, L.; He, X.; Guo, Y.; Shao, S.; Jiang, S. *Tetrahedron Lett.* **2007**, *48*, 4275.
- Mitra, A.; Chinta, J. P.; Rao, C. P. *Tetrahedron Lett.* **2010**, *51*, 139.
- Hariharan, M.; Karunakaran, S. C.; Ramaiah, D. *Org. Lett.* **2007**, *9*, 417.
- Hortala, M. A.; Fabbri, L.; Marcotte, N.; Stomeo, F.; Taglietti, A. *J. Am. Chem. Soc.* **2003**, *125*, 20.
- (a) Folmer-Andersen, J. F.; Lynch, V. M.; Anslyn, E. V. *Chem.-Eur. J.* **2005**, *11*, 5319; (b) Sun, S.-K.; Tu, K.-X.; Yan, X.-P. *Analyst* **2012**, *137*, 2124.
- Patel, G.; Menon, S. *Chem. Commun.* **2009**, 3563.
- Yang, R.; Wang, K.; Long, L.; Xiao, D.; Yang, X.; Tan, W. *Anal. Chem.* **2002**, *74*, 1088.
- (a) Huang, Z.; Du, J.; Zhang, J.; Yu, X.-Q.; Pu, L. *Chem. Commun.* **2012**, 3412; (b) Du, J.; Huang, Z.; Yu, X.-Q.; Pu, L. *Chem. Commun.* **2013**, 5399.
- Oliveira, E.; Santos, C.; Poeta, P.; Capelo, J. L.; Lodeiro, C. *Analyst* **2013**, *138*, 3642.
- Chen, X.; Wang, X.; Wang, S.; Shi, W.; Wang, K.; Ma, H. *Chem. Eur. J.* **2008**, *14*, 4719.
- Kubin, R. *J. Lumin.* **1983**, *27*, 455.
- Benesi, H. A.; Hildebrand, J. H. *J. Am. Chem. Soc.* **1949**, *71*, 2703.
- Gaussian 03, Rev. C.02; Gaussian Inc.: Wallingford, CT, 2004.

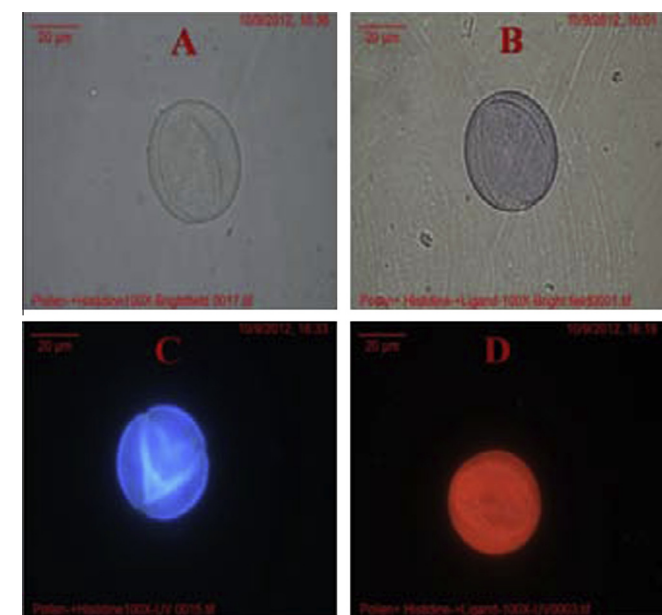


**Figure 6.** Bright field and fluorescence microscope images of pollen grains from *Tecomastans*. Top row (bright field): cells incubated with histidine (5 mM) for 1 h (A); cells treated with histidine and TARDHD (B). Bottom row (fluorescence image): cells incubated only with histidine (C) and cells treated with histidine and TARDHD (D).

Figure S13 (ESI) reveals that at low pH (below 4), the emission intensities of TARDHD and its histidine adduct are high, and the difference is very small, probably due to spiro lactam ring opening. Higher pH (above 9) favours the closed ring spiro lactam form. The difference of emission intensities being maximum in the pH range